RRH: CRETACEOUS/PALEOGENE BOUNDARY

LRH: LEIGHTON ET AL.

TIMING RECOVERY AFTER THE CRETACEOUS/PALEOGENE BOUNDARY: EVIDENCE FROM BRAZOS RIVER, TEXAS

ANDREW D. LEIGHTON[1], MALCOLM B. HART[1,4], CHRISTOPHER W. SMART[1], MELANIE J. LENG[2] AND MATTHEW HAMPTON[3]

[1]School of Geography, Earth and Environmental Sciences, Plymouth University, Plymouth, PL4 8AA, UK

[2]NERC Isotope Geosciences Facilities, British Geological Survey, Nottingham NG12 5GG, UK & School of Geography, University of Nottingham, University Park, Nottingham NG7 2RD, UK

[3]Network Stratigraphic Consulting Ltd, Harvest House, Cranborne Road, Potters Bar, Hertfordshire EN6 3JF, UK

[4]Correspondence author E-mail: mhart@plymouth.ac.uk

ABSTRACT

As part of an on-going re-assessment of the Cretaceous/Paleogene boundary in the Brazos River area, Falls County, Texas, a number of new exposures have been described. One of these, at Riverbank South, provides a near-continuous record of the lowermost Paleocene. It is from this succession that stable isotope analysis of bulk organic matter ($\delta^{13}C$ and C/N) and mono-specific samples of the benthic foraminifera *Lenticulina rotulata* Lamarck ($\delta^{18}O$ and $\delta^{13}C$) yields an orbitally-tuned stable isotope record, which allows the timing of events adjacent to the Cretaceous/Paleogene boundary to be determined. Using this cyclicity, it is suggested that the on-set of biotic recovery began ~40,000 years after the impact (near the base of Zone Pα) and that more significant recovery of planktic foraminifera and calcareous nannofossils began close to the base of Zone P1a, some 85,000–100,000 years post-impact. The data also appear to record the presence of the earliest Paleocene DAN-C2 and Lower C29n hyperthermal events and that these events appear to be an accentuated segment of this orbital cyclicity.

35

36 INTRODUCTION

37

38 The Cretaceous/Paleogene (K/Pg) mass extinction event is not the most severe of the
39 major extinction events in Earth's history but it is one of the most studied (Twitchett, 2006).
40 There were synchronous extinctions (Keller et al., 2009) in both the marine and terrestrial realms
41 including some invertebrates (e.g., ammonites), calcareous nannofossils, planktic foraminifera
42 and non-avian dinosaurs. A bolide impact at Chicxulub in the Yucatan Peninsula, Mexico, is
43 now generally accepted as a major cause of the extinction event (MacLeod et al., 2007), despite
44 on-going discussions (Schulte et al., 2010) regarding the timing of the extinctions and the
45 changes to global climate caused by the eruption of the Deccan volcanic centre in India (Adatte
46 et al., 2014; Keller, 2014; Punekar et al., 2014).
47 The K/Pg boundary on the Brazos River and its tributaries in Falls County, Texas (Fig. 1)
48 has been extensively studied (Hansen et al., 1987; Yancey, 1996; Keller et al., 2009; Adatte et
49 al., 2011; Hart et al., 2011, 2012) although there are on-going debates over the placement of the
50 boundary event in that area. Many of the discussions relate to the nature of the boundary
51 complex exposed in the Brazos River area, which has been interpreted as either tsunami deposits
52 associated with the Chicxulub impact (Bourgeois et al., 1988; Keller et al., 2003, 2009), a series
53 of storm deposits (Gale, 2006) or a succession of storm deposits resting on a tsunami-generated
54 erosion surface (Yancey, 1996; Hart et al., 2012; Yancey & Liu, 2013). At its base, the boundary
55 complex contains re-worked, impact-derived spherules, overlain by discrete sandstone bodies
56 (Hart et al., 2012) with hummocky cross-stratification, climbing ripples, complex bioturbation
57 and fossil-rich siltstone inter-beds. To date, investigations of this boundary have focused mainly

58 on exposures in the bed of the Brazos River close to the Rt. 413 bridge, the creeks (Darting
59 Minnow and Cottonmouth) or cored material. Recently, a new section on the Brazos riverbank,
60 which crops out between Cottonmouth and Darting Minnow creeks (8.5 km south of the Rt. 413
61 bridge), has been re-discovered and described (Plummer, 1926; Hart et al., 2012, figs. 2–4). This
62 exposure, known as River Bank South (RBS), is laterally continuous along a >100 m long cliff
63 and is currently the most complete exposure of the K/Pg boundary in the area at the present time
64 (Fig. 2). There have, however, been times between 1926 and 2011 when the outcrop was covered
65 by river-derived sediments.
66 The RBS succession exposes the uppermost part of the Corsicana Mudstone Formation
67 (uppermost Maastrichtian). The volcanic ash seen in Cottonmouth Creek, 45 cm below the base
68 of the 'Event Bed' (Keller et al.,2007; Hart et al., 2012) has not been recorded despite quite
69 extensive clearance of the outcrop. This volcanic ash, fully documented by Hart et al. (2012, p.
70 75–77) has been recorded within the Corsicana Mudstone Formation just north of the Rt. 413
71 bridge at a location described as River Bank North (RBN on Fig. 1). The thickness of the
72 Corsicana Mudstones between the volcanic ash and the tsunami-generated erosion surface is
73 variable, as would be expected below such an erosive surface. The conglomerate of re-deposited
74 calcareous mudstone nodules that marks the base of the 'Event Bed' succession in the bed of the
75 Brazos River immediately downstream of the Rt. 413 bridge is also indicative of the levels of
76 down-cutting by the tsunami. In Darting Minnow Creek the 'Event Bed' is present in the
77 waterfall succession but, traced downstream, the Maastrichtian mudstones are directly overlain
78 by Paleocene strata with the level of the 'Event Bed' represented by only an erosion surface. The
79 absence of the 'Event Bed' was also recorded in the nearby Mullinax 3 core (Adatte et al., 2011;
80 Hart et al., 2012). This level of field investigation and understanding is required prior to the

careful collection of representative suites of samples from the various localities and the subsequent micropaleontological investigations.

METHODOLOGY

Planktic foraminifera have been extensively studied (Keller, 1989; Keller et al., 2009; Abramovich et al., 2011) in this area and they clearly demonstrate the typical K/Pg mass extinction pattern. Fewer investigations of benthic foraminifera have been undertaken (Plummer, 1926, 1931; Cushman, 1946; Hart et al., 2011; Leighton, 2014), even though they are highly diverse and abundant throughout the K/Pg boundary succession. Figure 3 shows the lithostratigraphy, nature of the sediments and some of the more important benthic foraminifera. This assemblage is typical of the Gulf Coastal Plain area (Plummer, 1926, 1931; Cushman, 1946; Olsson et al., 1996; Culver, 2003; Schulte & Speijer, 2009). As indicated by Hart et al. (2011, 2012), both the latest Maastrichtian and earliest Paleocene assemblages are typical of an inner to mid-shelf setting with a water depth of 50–100 m based on the analysis of morphotypes (see Koutsoukos & Hart, 1990). This so-called 'Midway-type assemblage' (Berggren & Aubert, 1975) is in contrast to the deeper-water 'Velasco-type assemblage' (Schnitker, 1979) that has been described from northeast Mexico (Alegret & Thomas, 2001 and references therein).

Here we report stable isotope ratios obtained from the benthic species *Lenticulina rotulata* Lamarck, an epifaunal/semi-infaunal taxon (Koutsoukos & Hart, 1990) that is abundant throughout the succession and has been used by other authors (Keller et al., 2009; Adatte et al., 2011) for stable isotope analysis at other K/Pg boundary locations. Specimens for the stable isotope analysis were obtained by normal micropaleontological processing techniques. The bulk

104 sediment was air dried, weighed and then soaked in white spirit (Stoddart Spirit) for ~4 hours,
105 after which the excess white spirit was removed by filtering. Samples were then immersed in de-
106 ionised water for ~12 hours before washing through a 45 μm sieve, and then dried in an oven at
107 20°C. Once dry, the >45 μm residues were dry sieved into the >500 μm, 500–250 μm, 250–150
108 μm and 150–45 μm size fractions. If the samples were not fully disaggregated the whole process
109 was repeated 2 or even 3 times. All samples were processed in stratigraphical order.
110 Individual specimens of *L. rotulata* from three different size fractions were analysed to
111 assess the isotopic variations with specimen size (= growth or ontogeny). Specimens from the
112 >500 μm, 500–250 μm and 250–150 μm size fractions were checked by both optical and electron
113 microscopy for evidence of re-crystallization or chamber infilling. Clean specimens were
114 weighed, as approximately 15–100 mg were required for the isotope analysis. For the >500 μm
115 size fraction, this equated to 2–3 individuals, while 4–6 and 9–14 individuals were needed from
116 the 500–250 μm, and 250–150 μm fractions respectively. Measurements of $\Delta^{13}C$ and $\delta^{18}O$ were
117 performed on a GV IsoPrime mass spectrometer plus Multiprep device, located in the National
118 Isotope Geosciences Laboratory (NIGL), Keyworth, Nottingham. Isotope values ($\delta^{13}C$, $\delta^{18}O$) are
119 reported as per mille (‰) deviations of the isotopic ratios ($^{13}C/^{12}C$, $^{18}O/^{16}O$) calculated to the
120 VPDB scale using a within-run laboratory standard calibrated against NBS standards. Analytical
121 reproducibility of the standard calcite (KCM) is < 0.1‰ for $\delta^{13}C$ and $\delta^{18}O$.
122 After an acid wash to remove any carbonate material, $\delta^{13}C$ and C/N were measured on
123 the organic material by combustion in a Costech Elemental Analyser (EA) on-line to a VG Triple
124 Trap and Optima dual-inlet mass spectrometer (also located at NIGL). Values of $\delta^{13}C$ were
125 calculated to the VPDB scale using a within-run laboratory standards calibrated against NBS18,
126 NBS-19 and NBS22. Replicate analysis of well-mixed samples indicated a precision of + <0.1‰

(1 SD). Ratios of C/N were calibrated against an Acetanilide standard. Replicate analysis of well-mixed samples indicated a precision of + <0.1.

RESULTS

The stable isotope data from *L. rotulata* are shown in Figure 4. As there is a significant degree of reworking in the lowermost Paleocene, it is possible that the first 50 cm of the Paleocene *may* include a re-worked signal from the Maastrichtian, *despite* the excellent preservation. It is evident that the large $\delta^{13}C$ negative excursion that is often recorded immediately above the K/Pg boundary (Fig. 5) is not present in the RBS section (see Martinez-Ruiz et al., 1994; Hart et al., 2005, fig. 10; Lamolda et al., 2016, fig. 7; Hart et al., 2016, fig. 4). This is unsurprising as the global, post-impact iridium anomaly is also absent from this succession (Gertsch & Keller, 2012).

There is a full discussion of the K/Pg boundary at River Bank South given by Hart et al. (2012). Following the agreed definition of the Global Stratotype Section and Point (GSSP) provided by Molina et al. (2006), the boundary is the erosion surface generated by the tsunami that resulted from the Chicxulub impact, with the overlying spherule bed and storm-derived sandstones and siltstones representing the lowermost Paleocene. In more distal areas (from the impact) such as Stevns Klint (Denmark), the Bottacione Gorge and Contessa Highway successions near Gubbio (Italy), Gams (Austria), El Kef (Tunisia), Agost (Spain) and Caravaca (Spain) the boundary hiatus is immediately overlain by sediments containing the iridium anomaly and the negative $\delta^{13}C$ isotope excursion (see, for example, Lamolda et al., 2016, fig. 7), neither of which are recorded in the Brazos River successions.

In the RBS succession, a series of gradually increasing, cyclical (?), stable isotope excursions are recorded up-section into the Paleocene (Fig. 4). The >500 μm signal records these excursions well, but the amplitude of each excursion increases as the size and, therefore, maturity, of the *L. rotulata* specimens decreases. This indicates that the size (= age) of the benthic foraminifera test is inversely proportional to the $\delta^{18}O$ and $\delta^{13}C$ signals. The amplitude of the cyclicity in these excursions increases from the K/Pg boundary to within Zone P1a, where the largest excursions (~6‰ and >5‰ in $\delta^{18}O$ and $\delta^{13}C$ respectively) in the smallest size fraction are recorded. The excursions occur in all of the size fractions in the same interval, indicating that the isotope signal appears to be genuine.

Cross-plots of $\delta^{18}O$ and $\delta^{13}C$ are often used extensively in paleoceanography (e.g., Wendler et al., 2013) to identify both benthic and planktic foraminifera niches (e.g., Birch et al., 2013 and references therein). In our case, only data from a single benthic taxon is used and any scatter, therefore, shows only the variability of the stable isotope signal with the size of specimens analysed (= growth).

The bulk organic $\delta^{13}C_{org}$ is similar to the benthic foraminiferal $\delta^{13}C_{carbonate}$ especially around the major excursions in Zone P1a (Fig. 5). Bulk $\delta^{13}C_{org}$ shows a negative excursion of >1‰, followed by a positive excursion of >1‰. Bulk $\delta^{13}C_{org}$ shows a cyclical pattern of positive and negative excursions, the magnitude of which increases up-section, similar to benthic foraminiferal $\delta^{13}C_{carbonate}$. The carbon/nitrogen (C/N) ratio increases to >10 in this interval which would normally be interpreted as a greater contribution of terrestrial organic material (Fig. 5; see Sampei & Matsumoto, 2001 and Lamb et al.,2007).

There is a variable response in the foraminifera >500 μm, 500–250 μm and 250–150 μm size fraction $\delta^{18}O$ data, with the greatest variation within the smallest (usually the more juvenile)

specimens. This ontogenetic variation in stable isotope data in benthic foraminifera has been reported before using extant material (Schumacher et al., 2010) from the Indian Ocean, where the variation was attributed to the infaunal mode of life, with juveniles residing at a greater depth in the sediment than the larger adults. Ishimura et al. (2012) have confirmed this variation, although they used the weight (i.e., calcification) of the specimens rather than overall dimensions. In their study of living foraminifera, the lightest and, therefore, the youngest and – though not discussed – the smallest forms recorded the largest negative excursions. Wendler et al. (2013), reported a large variation in *Lenticulina* spp. stable isotope data from the Turonian (Wendler et al., 2013, fig. 6) and this was attributed to the opportunistic life-style of the genus (*op. cit*., p. 22). These authors suggest that, for most of the benthic taxa used in their analysis, between 1 and 22 specimens were required in order to perform the stable isotope analysis. If *Lenticulina* spp. are recording significant stable isotope variability with size (both ontogenetic change and changes in life position *vis á vis* the sediment surface) then this might explain the variability recorded by Wendler et al. (2013, p. 6). As many other authors (Keller et al., 2007, 2009) have used this genus from a range of size fractions their data may have been compromised by this ontogenetic variability. This relationship has previously been described from planktic foraminifera (Bornemann & Norris, 2007; Birch et al., 2013), where individuals are known to change their position in the water column during ontogeny, but has rarely been reported in studies of benthic foraminifera.

Whilst there is a close agreement between the results of all three size fractions, it is the 250–150 μm size fraction (juveniles) that displays the greatest variability in the $\delta^{18}O$ data (Fig. 4). These results indicate that there is a clear variation in $\delta^{18}O$ and $\delta^{13}C$ with size and that comparisons with data generated from 'bulk' or randomly selected individuals may be invalid.

196 The graphs in Figure 4 show that only a profile based on standardised samples can be used in a
197 reliable way to determine events. The key features of the stable isotope data are presented below.
198 The lowermost Paleocene 'large' negative $\delta^{13}C$ excursion (Hart et al., 2005, fig. 10;
199 Schulte et al., 2010; Hart et al., 2016, fig. 4; Lamolda et al., 2016, fig. 7) is not evident (except
200 perhaps in the fine fraction data: Fig. 5). This is because the reworked spherule-rich bed and the
201 sandstones of the 'Event Bed' represent a disturbed environment in which the stable isotope
202 signal has been lost by erosion or completely masked by sediment mixing. The pattern of $\delta^{18}O$
203 and $\delta^{13}C$ excursions above the 'Event Bed' appears cyclical and probably represents an orbital
204 forcing. A record of orbital cyclicity is well-known in the Maastrichtian (Hart et al., 2005, fig. 9;
205 Batenberg et al., 2012, 2014) and Paleocene (Zachos et al., 2010; Westerhold et al., 2012) and
206 the cyclicity observed in our RBS succession is almost certainly that of the 21kyr precession
207 signal. Although no obvious sedimentary cycles are observed in the lowermost Paleocene
208 deposits of Texas (Fig. 2), there are distinctive carbonate-mudstone cycles recorded in the coeval
209 Lower Paleocene sediments of the Braggs, Mussel Creek (Hart et al., 2013, fig. 7), Miller's Ferry
210 (Olsson et al., 1996) and Moscow Landing (Hart et al., 2013, fig. 12) successions in Alabama.
211
212 TIMING OF EVENTS
213
214 In the chalks of the Sigerslev Member (Surlyk et al., 2006) exposed in the Stevns Klint
215 succession, the stable isotope data (Hart et al., 2005, fig. 10) appear to record a precessional
216 cyclicity, which was also recorded in the Maastricht chalk succession of the Netherlands
217 (Schiøler et al., 1997) and in the Maastrichtian successions on the north coast of Spain
218 (Batenberg et al., 2012, 2014). The 'Grey Chalk' (= Højerup Member) of the Stevns Klint

219 succession, which displays visible signs of sediment transport and the formation of 'mounds' on
220 the Maastrichtian sea floor, records no cyclicity as a result of sediment mixing. The overlying
221 Fish Clay (= Fiskeler Member), however, records (Hart et al., 2016, fig. 4) the characteristic,
222 negative $\delta^{13}C$ excursion (see Molina et al., 2006) and a number of other $\delta^{13}C$ excursions that
223 diminish in magnitude up-section (see Martinez-Ruiz et al., 1994). The total thickness of the Fish
224 Clay may, if these are precessional cycles, represent 40,000 – 60,000 years. This interval of time
225 is represented by only <50 cm of sediment (after compaction), implying a remarkably slow rate
226 of sedimentation. This is, however, to be expected as – in the chalk sea of northwest Europe – a
227 loss of calcareous nannofossils and planktic foraminifera would significantly reduce the
228 sediment supply. The background supply of siliciclastic sediment (largely clays) normally
229 represents <1% of uppermost Cretaceous chalks in north-west Europe (Hancock, 1976) and the
230 loss of carbonate sediment supply following the K/Pg mass extinction event explains the reduced
231 sedimentation rate. The Fish Clay contains a diverse and abundant assemblage of
232 dinoflagellatecysts (Hansen, 1977; Hultberg, 1985, 1986, 1987; Hultberg & Malmgren, 1987),
233 but this abundance must also be viewed in the context of the reduced sedimentation rate.
234 In Texas, however, the dominant sediment supply is siliciclastic and the stable isotope
235 data (Fig. 4) do not show the same levels of condensation, despite a similar loss of calcareous
236 nannofossils and planktic foraminifera at the level of the K/Pg extinction event. The large $\delta^{13}C$
237 negative excursion is missing and there are, therefore, ~2 excursions prior to the P0/Pα
238 boundary. This indicates ~40,000 years of elapsed time between the extinction event and the
239 onset of 'recovery'. Berggren & Pearson (2005) have also indicated ~30,000 years for the
240 duration of Zone P0. As there are a further 2–3 cycles to the Pα/P1a boundary (Fig. 4), this
241 places the on-set of a more comprehensive recovery of the plankton at ~80,000–100,000 years.

242 At the level of the Middle Sandstone Bed (MSB) and the Dirty Sandstone Bed (DSB) the
243 benthic foraminifera are at their most diverse (Fig. 3) with large specimens recorded. Many of
244 these nodosariids are exceptionally long and, as the apical spine and the aperture are often
245 present, unlikely to have suffered any disturbance or transport. The presence of these large
246 specimens was noted by Plummer (1926) as being a particular characteristic of the RBS section.
247 Following the models of Emery & Myers (1996, fig. 6.14) and Oxford et al. (2000, 2004), this
248 would suggest that the MSB/DSB interval represents a zone of maximum flooding, which may
249 contribute to the increased $\delta^{13}C$ peak. There is also a peak in the $\delta^{13}C_{organic}$ record (Fig. 5), which
250 may indicate a greater supply of terrestrial organic material and increased surface run-off from
251 the land.
252
253 PALEOCENE HYPERTHERMAL EVENTS
254
255 The Paleocene world was characterised by a continuing greenhouse condition and, within
256 it, there are a number of significant – but transient – hyperthermal events (Bralower et al., 2002;
257 Speijer, 2003; Petrizzo, 2005; Bernaola et al., 2007; Quillévéré et al., 2008; Bornemann et al.,
258 2009; Coccioni et al., 2010). Whilst the most prominent is the Paleocene–Eocene Thermal
259 Maximum or PETM (Zachos et al., 2001, 2010), earlier events are also quite significant and, in
260 carbonate-rich sediments, are associated with a drop in carbonate production and/or enhanced
261 dissolution. The DAN-C2 and Lower C29n events (Coccioni et al., 2010) have been identified in
262 the Contessa Highway section (Gubbio, Italy) and a small number of ODP/DSDP sites
263 (Quillévéré et al., 2008). None of these locations are in a shallow-water, mid-shelf environment,
264 comparable with the Brazos River area. In the RBS succession the maximum $\delta^{13}C$ excursion

265 appears to be coeval with the Lower C29n event while the Dan-C2 event (represented by the
266 upper Pα and lower P1a zones) is less pronounced.
267 The significant negative $\delta^{18}O$ and $\delta^{13}C$ excursion near the NP1/NP2 boundary
268 approximately 2.5 m above the K/Pg boundary represents a possible <6°C warming that is
269 relatively short-lived. This appears to be coeval with the Lower C29n hyperthermal event
270 (Coccioni et al., 2010) while a smaller, but still significant, negative $\delta^{18}O$ and $\delta^{13}C$ excursion
271 below this near the Pα/P1a boundary appears to be coeval with the DAN-C2 hyperthermal event.
272 The DAN-C2 hyperthermal event (Quillévéré et al., 2008; Coccioni et al., 2010) occurs within
273 the lower P1a and NP1 biozones, while the Lower C29n hyperthermal event occurs within the
274 uppermost part of the NP1 calcareous nannofossil biozone and within the P1a planktic
275 foraminiferal biozone. The hyperthermal events at Contessa Highway (Coccioni et al., 2010)
276 appear coeval with the timing of the excursions in the RBS section as the biostratigraphy is well-
277 constrained. The biostratigraphy within the RBS section is reliable and accurate, with the
278 calcareous nannofossil data based on the same samples as those used in the analysis of the
279 benthic and planktic foraminifera and the stable isotope analyses. The distribution of the planktic
280 foraminifera in the RBS succession is exactly comparable to that recorded in the Brazos-1
281 section by Liu (pers. comm., 2012, 2013) and the Brazos River outcrop immediately south of the
282 Rt. 413 bridge. The distribution of taxa is also in agreement with that recorded in the Mullinax-1
283 borehole (Abramovich et al., 2011; Keller & Adatte, 2011 and papers cited therein), though our
284 placing of the K/Pg boundary is different to that recorded by these authors. The calcareous
285 nannofossil data allow the placing of NP1 and NP2, with direct comparisons to the successions
286 in Agost (Lamolda et al., 2016), Caravaca (Lamolda et al., 2005), El Kef (Pospichal, 1994) and
287 Elles (Gardin, 2002). The magnitude of the stable isotopic excursions recorded in the Brazos

River area are larger than those observed near Gubbio (Coccioni et al., 2010), although this can be attributed to the use of species-specific benthic foraminifera within this study rather than bulk rock samples.

The $\delta^{13}C_{organic}$ isotope data (Fig. 5) are in close agreement with the species-specific foraminiferal isotope data, with the $\delta^{13}C_{organic}$ signal closely reflecting the excursions of the species-specific $\delta^{13}C_{carbonate}$ isotope data. This indicates that the carbon source for both the foraminifera and the sediments ($\delta^{13}C_{organic}$ and $\delta^{13}C_{carbonate}$) is the same. An increase in the C/N ratio >10 indicates a more terrestrial origin for organic material (Fig. 5). The marked increase in the C/N ratio coincides with the marked negative $\delta^{13}C$ excursion of the foraminiferal isotopic data and suggests that there was a greater supply of terrestrial plant material and increased surface run-off from the land onto the shelf. This mechanism could also account for the fluctuations of the $\delta^{18}O$ isotope signal as this could be marking an increase of freshwater into the system and, therefore, much lighter isotopic values. Increased surface run-off from the land, as a result of hydrological changes, is a particular feature that often characterizes hyperthermal events (see Manners et al., 2013, and references therein), so the interpretation of increased freshwater input into the Brazos River area supports this conclusion.

The general warming recorded by the DAN-C2 and Lower C29n events (Coccioni et al., 2010) appears to be associated with the interval of time close to the last of the eruption phases of the Deccan Plateau (Chenet et al., 2007, 2009), although there is an on-going re-evaluation of the ages of the Deccan volcanics (e.g., Schoene et al., 2015). The timing of the hyperthermal event(s) in the Brazos River area suggests that the DAN-C2 and Lower C29n event may be more widespread than previously suggested. The stable isotope data from the Brazos River area may be astronomically tuned, a feature of the DAN-C2 event (Quillévéré et al., 2008). An

311 astronomical signal has also been suggested (Jolley et al., 2011; Gilmour et al., 2012, 2013,
312 2014) following an analysis of the sediments within the Boltysh impact crater in Ukraine. There
313 are four climate-induced cycles (Gilmour et al., 2013, 2014) between the K/Pg boundary and
314 what has been identified as the DAN-C2 event. If this cyclicity, and the DAN-C2 event (and
315 Lower C29n event), are confirmed from terrestrial, shallow marine (Brazos River area) and
316 deeper marine successions, then these events are comparable to other Paleogene hyperthermal
317 events that are recorded globally and from a wide range of environments (both terrestrial and
318 marine).
319
320 CONCLUSIONS
321
322 Stable isotope data derived from size-controlled samples of *Lenticulina rotulata* Lamarck
323 across the K/Pg boundary in the Brazos River area, Texas, indicate that early recovery began
324 ~40,000 years post-impact and that a more significant recovery was under-way by 80,000–
325 100,000 years post-impact. The data also suggest that the DAN-C2 and Lower C29n
326 hyperthermal events have been detected in the mid-shelf environment represented by the
327 sediments of the Kincaid Formation, Brazos River area, Falls County, Texas. These events
328 appear to be coeval with those identified from the Contessa Highway K/Pg section in Italy, and
329 occur at the same stratigraphic level as determined by both calcareous nannofossil and planktic
330 foraminferal biozonation schemes. The variation in $\delta^{18}O$ and $\delta^{13}C$ recorded in the various size
331 fractions of the mono-specific samples used in our investigation raises issues for stable isotope
332 data derived from variously-sized foraminifera or samples of mixed benthic assemblages. The
333 data do, however, indicate that fossil material is showing stable isotope variations in line with

those recorded in modern (living) foraminifera. The stable isotopic signal from the Brazos River area indicates an increased amount of surface run-off (freshwater input) in the early Paleocene. The increased surface run-off, hyperthermal events and bulk organic $\delta^{13}C$ geochemical signals indicate that the earliest Paleocene immediately after the K/Pg boundary event was a period of climatic instability and fluctuating environmental parameters.

ACKNOWLEDGMENTS

ADL acknowledges receipt of a Plymouth University Scholarship to support his PhD research (2009–2013). The authors also acknowledge financial support from Plymouth University, the Geological Society of London (MBH) and Shell Exploration & Production, Houston (MBH/ADL). Mr and Mrs Mullinax, owners of the Brazos Rose Ranch, are also thanked for their hospitality and un-paralleled access to their property. Prof. Tom Yancey (Texas A&M University, USA) and Prof. Rodolfo Coccioni (Urbino, Italy) are also thanked for helpful and constructive discussions. The authors acknowledge the helpful comments (and criticisms) of two reviewers that have prompted a number of improvements to the final version of the paper. Mr Tim Absalom (Plymouth University Geomapping Unit) is thanked for his assistance with some of the figures.

REFERENCES

Abramovich, S., Keller, G., Berner, Z., Cymbalista, M., and Rak, C., 2011, Maastrichtian planktic foraminiferal biostratigraphy and paleoenvironment of Brazos River, Falls

County, Texas, USA, *in* Keller, G., and Adatte, T., (eds.), The end-Cretaceous mass extinction and the Chicxulub impact in Texas: SEPM Special Publication, v. 100, p. 123–156.

Adatte, T., Keller, G., and Baum, G. R., 2011, Age and origin of the Chicxulub impact and sandstone complex, Brazos River, Texas: Evidence from lithostratigraphy and sedimentology, *in* Keller, G., and Adatte, T. (eds.), The end-Cretaceous mass extinction and the Chicxulub impact in Texas: SEPM Special Publication, v. 100, p. 43–80.

Adatte, T., Fantasia, A., Samant, B., Mohabey, D., Font, E. Keller, G., Khozyem, H., and Gertsch, B., 2014, Deccan volcanism: a main trigger of environmental changes leading to the K/Pg mass extinction?: Communicações Geológicas, v. 101, Especial lll, p. 1435–1437.

Alegret, L., and Thomas, E., 2001, Upper Cretaceous and lower Paleogene benthic foraminifera from northeastern Mexico: Micropaleontology, v. 47, p. 269–316.

Batenberg, S. J., Sprovieri, M., Gale, A. S., Hilgen, F. J., Hüsing, S., Laskar, J., Liebrand, D., Lirer, F., Orue-Extebarria, X., Pelosi, N., and Smit, J., 2012, Cyclostratigraphy and astronomical tuning of the Late Maastrichtian at Zumaia (Basque country, Northern Spain): Earth and Planetary Science Letters, v. 359–360, p. 264–278.

Batenberg, S. J., Gale, A. S., Sprovieri, M., Hilgen, F. J., Thibault, N., Boussaha, M., Orue-Etxebarria, X., 2014, An astronomical time scale for the Maastrichtian based on the Zumaia and Sopelana sections (Basque country, northern Spain): Journal of the Geological Society, London, v. 171, p. 165–180.

Berggren, W. A., and Aubert, J., 1975, Paleocene benthonic foraminiferal biostratigraphy, paleobiogeography and paleoecology of Atlantic-Tethyan regions: Midway-type fauna: Palaeogeography, Palaeoclimatology, Palaeoecology, v. 18, p. 73–192.

Berggren, W. A., and Pearson, P. N., 2005, A revised tropical to subtropical Paleogene planktonic foraminiferal zonation: Journal of Foraminiferal Research, v. 35, p. 279–298.

Bernaola, G., Baceta, J. I., Orue-Extebarria, X., Alegret, L., Martin-Rubio, M., Arostegui, J., and Dinarès-Turell, J., 2007, Evidence of an abrupt environmental disruption during the mid-Paleocene biotic event (Zumaia section, western Pyrenees): Geological Society of America Bulletin, v. 119, p. 785–795.

Birch, H., Coxall, H. K., Pearson, P. N., Kroon, D., O'Regan, M., 2013, Planktonic foraminifera stable isotopes and water column structure: Disentangling ecological signals: Marine Micropaleontology, v. 101, p. 127–145.

Bornemann, A., and Norris, R. D., 2007, Size-related stable isotope changes in Late Cretaceous planktic foraminifera: Implications for paleoecology and photosymbiosis: Marine Micropaleontology, v. 29, p. 32–42.

Bornemann, A., Schulte, P., Sprong, J., Steurbaut, E., Youssef, M., and Speijer, R. P., 2009, Latest Danian carbon isotope anomaly and associated environmental change in the Southern Tethys (Nile basin, Egypt): Journal of the Geological Society, London, v. 166, p. 135–142.

Bourgeois, J., Hansen, T. A., Wiberg, P. L., and Kauffman, E. G., 1988, A tsunami deposit at the Cretaceous-Tertiary boundary in Texas: Science, v. 241, p. 567–570.

399 Bralower, T. J., Premoli Silva, I., and Malone, M. J., 2002, New evidence for abrupt climate
400 change in the Cretaceous and Paleogene: an Ocean Drilling Program expedition to
401 Shatsky Rise, northwest Pacific: GSA Today, v. 12, p. 4–10.
402 Chenet, A. L., Quidelleur, X., Fluteau, F., Courtillot, V., and Bajpai, S., 2007, $^{40}K–^{40}Ar$ dating of
403 the Main Deccan large igneous province: Further evidence of KTB age and short
404 duration: Earth and Planetary Science Letters, v. 263, p. 1–15.
405 Chenet, A. L., Courtillot, V., Fluteau, F., Gerard, M., Quidelleur, X., Khadri, S. F. R., Subbaro,
406 K. V., and Thordarson, T., 2009, Determination of rapid Deccan eruptions across the
407 Cretaceous-Tertiary boundary using paleomagnetic secular variation: 2. Constraints from
408 analysis of eight new sections and synthesis for a 3500 m-thick composite section:
409 Journal of Geophysical Research, v. 114, B06103, DOI:10.1029/2008JB005644
410 Coccioni, R., Frontalini, F., Bancalà, G., Fornaciari, E., Jovane, L., and Sprovieri, M., 2010, The
411 Dan-C2 hyperthermal event at Gubbio (Italy): Global implications, environmental
412 effects, and cause(s): Earth and Planetary Science Letters, v. 297, p. 298–305.
413 Culver, S. J.,2003, Benthic foraminifera across the Cretaceous–Tertiary (K–T) boundary: A
414 review: Marine Micropaleontology, v. 47, p. 177–226.
415 Cushman, J. A., 1946, Upper Cretaceous foraminifera of the Gulf Coastal region of the United
416 States and adjacent areas: United States Geological Survey, Professional Paper, no. 206,
417 241 p.
418 Emery, D., and Myers, K. J, 1996, Sequence Stratigraphy: Blackwell Science, Oxford,297 p.
419 Gale, A. S., 2006, The Cretaceous-Palaeogene boundary on the Brazos River, Falls County,
420 Texas: Is there evidence for impact-induced tsunami sedimentation?: Proceedings of the
421 Geologists' Association, London, v. 117, p. 173–185.

Gardin, S., 2002, Late Maastrichtian to early Danian calcareous nannofossils at Elles (Northwest Tunisia). A tale of one million years across the K-T boundary: Palaeogeography, Palaeoclimatology, Palaeoecology, v. 178, p. 211–231.

Gertsch, B., and Keller, G., 2012, Platinum group element (PGE) geochemistry of Brazos sections, Texas, USA, *in* Keller, G., and Adatte, T. (eds.), The end-Cretaceous mass extinction and the Chicxulub impact in Texas, SEPM Special Publication, v. 100, p. 227–249.

Gilmour, I., Jolley, D. J. W., Daley, R. J., Kelley, S. P., and Gilmour, M. A., 2012, A complete high resolution record of the Dan-C2 hyperthermal event in the lacustrine sediments of the Boltysh Impact Crater. Geophysical Research Abstracts, v. 14, EGU2012-7870-2 [abstract].

Gilmour, I., Gilmour, M., Jolley, D., Kelly, S., Kemp, D., Daly, R., and Watson, J., 2013, A high-resolution nonmarine record of an early Danian hypothermal event, Boltysh crater, Ukraine: Geology, v. 41, p. 783–786.

Gilmour, I., Jolley, D., Kemp, D., Kelley, S., Gilmour, M., Daly, R., and Widdowson, M., 2014, The early Danian hyperthermal event at Boltysh (Ukraine): Relation to Cretaceous-Paleogene boundary events, *in* Keller, G., and Kerr, A. C. (eds.), Volcanism, Impacts, and Mass Extinctions: Causes and Effects: Geological Society of America, Special Paper No. 505, p. 133–146.

Hancock, J. M., 1976, The petrology of the chalk: Proceedings of the Geologists' Association, London, v. 86, p. 499–535 [for 1975].

443 Hansen, J. M., 1977, Dinoflagellate stratigraphy and echinoid distribution in Upper
444 Maastrichtian and Danian deposits from Denmark: Bulletin of the Geological Society of
445 Denmark, v. 26, p. 1–26.
446 Hansen, T. A., Farrand, B. R., Montgomery, H. A., Billman, H. G., and Blechschmidt, G., 1987,
447 Sedimentology and extinction patterns across the Cretaceous-Tertiary boundary interval
448 in east Texas: Cretaceous Research, v. 8, p. 229–252.
449 Hart, M. B., Feist, S. E., Håkansson, E., Heinburg, C., Price, G. D., Smart, C. W., and
450 Watkinson, M. P., 2005, The Cretaceous-Palaeogene boundary succession at Stevns
451 Klint, Denmark: Foraminifers and stable isotope stratigraphy: Palaeogeography,
452 Palaeoclimatology, Palaeoecology, v. 224, p. 6–26.
453 Hart, M. B., Searle, S. R., Feist, S. E., Leighton, A. D., Price, G. D., Smart, S. W., and Twitchett,
454 R. J., 2011, The distribution of benthic foraminifera across the Cretaceous-Paleogene
455 boundary in Texas (Brazos River) and Denmark (Stevns Klint), *in* Keller, G., and Adatte,
456 T. (eds.), The end-Cretaceous mass extinction and the Chicxulub impact in Texas: SEPM
457 Special Publication, v. 100, p. 179–196.
458 Hart, M. B., Yancey, T. E., Leighton, A. D., Miller, B., Liu, C., Smart, C. W., and Twitchett, R.
459 J., 2012, The Cretaceous-Paleogene boundary on the Brazos River, Texas: new
460 stratigraphic sections and revised interpretations: Journal of the Gulf Coast Association
461 of Geological Societies, v. 1, p. 69–80.
462 Hart, M. B., Harries, P. J., and Cárdenas, A. L., 2013, The Cretaceous/Paleogene boundary
463 events in the Gulf Coast: Comparisons between Alabama and Texas: Gulf Coast
464 Association of Geological Societies, Transactions, v. 63, p. 235–255.

Hart, M. B., FitzPatrick, M. E. J., and Smart, C. W., 2016, The Cretaceous/Paleogene boundary: Foraminifera, sea grasses, sea level change and sequence stratigraphy: Palaeogeography, Palaeoclimatology, Palaeoecology, v. 441, p. 420–429.

Hultberg, S. U., 1985, Dinoflagellate studies of the Upper Maastrichtian and Danian in southern Scandinavia: University of Stockholm, unpublished PhD Thesis, 189p.

Hultberg, S. U., 1986, Danian dinoflagellate zonation, the C-T boundary and the stratigraphical position of the fish clay in southern Scandinavia: Journal of Micropalaeontology, v. 5, p. 37–47.

Hultberg, S. U., 1987, Palynological evidence for a diachronous low-salinity event in the C-T boundary clay at Stevns Klint, Denmark: Journal of Micropalaeontology, v. 6, p. 35–40.

Hultberg, S. U., and Malmgren, B. A., 1987, Quantitative biostratigraphy based on Late Maastrichtian dinoflagellates and planktonic foraminifera from Southern Scandinavia: Cretaceous Research, v. 8, p. 211–228.

Ishimura, T., Tsunogai, U., Hasegawa, S., Nakagawa, F., Oi, T., Kitazato, H., Suga, H., and Toyofuku, T., 2012, Variation is stable carbon and oxygen isotopes of individual benthic foraminifera: Tracers for quantifying the magnitude of isotopic disequilibrium: Biogeosciences, v. 9, p. 4353–4367.

Jolley, D., Gilmour, I., Gurov, E., Kelley, S., and Watson, J., 2011, Two large meteorite impacts at the Cretaceous-Paleogene boundary: Geology, v. 38, p. 835–838.

Keller, G., 1989, Extended Cretaceous/Tertiary boundary extinctions and delayed population change in planktonic foraminifera from Brazos River, Texas: Paleoceanography, v. 4, p. 287–332.

487 Keller, G., 2014, Deccan volcanism, the Chicxulub impact, and the end-Cretaceous mass
488 extinctions: Coincidences? Cause and effect? *in* Keller, G., and Kerr, A. C. (eds.),
489 Volcanism, Impacts, and Mass Extinctions: Causes and Effects: Geological Society of
490 America, Special Paper No. 505, p. 57–90.
491 Keller, G., Stinnesbeck, W., Adatte, T., and Stüben, D., 2003, Multiple impacts across the
492 Cretaceous-Tertiary boundary: Earth Science Reviews, v. 62, p. 327–363.
493 Keller, G., Adatte, T., Berner, Z., Harting, M., Baum, G., Prauss, M., Tantawy, A., and Stüben,
494 D., 2007, Chicxulub impact predates K–T boundary: New evidence from Brazos, Texas:
495 Earth and Planetary Science Letters, v. 255, p. 339–356.
496 Keller, G., Adatte, T., Berner, Z., Pardo, A., and Lopez-Oliva, L., 2009, Age and biotic effects of
497 the Chicxulub impact in Mexico: Journal of the Geological Society, London, v. 166, p.
498 393–411.
499 Koutsoukos, E. A. M., and Hart, M. B., 1990, Cretaceous foraminiferal morphogroup
500 distribution patterns, palaeocommunities and trophic structures: A case study from the
501 Sergipe Basin, Brazil: Transactions of the Royal Society, Edinburgh, Earth Sciences, v.
502 81, p. 221–246.
503 Lamb, A. L., Vane, C. H., Wilson, G. P., Rees, J. G., and Moss-Hayes, V. L., 2007, Assessing
504 $\delta^{13}C$ and C/N ratios from organic material in archived cores as Holocene sea level and
505 palaeoenvironmental indicators in the Humber Estuary, UK: Marine Geology, v. 244, p.
506 109–128.
507 Lamolda, M. A., Melinte, M. C., and Kaiho, K., 2005, Nannofloral extinction and survivorship
508 across the K-Pg boundary at Caravaca, southeastern Spain. Palaeogeography,
509 Palaeoclimatology, Palaeoecology, v. 224, p. 27–52.

510 Lamolda, M. A., Melinte-Dobrinescu, M. C., and Kaiho, K., 2016, Calcareous nannoplankton
511 assemblage changes linked to paleoenvironmental deterioration and recovery across the
512 Cretaceous-Paleogene boundary in the Betic Cordillera (Agost, Spain): Palaeogeography,
513 Palaeoclimatology, Palaeoecology, v. 441, p. 438–452.
514 Leighton, A. D., 2014, Benthic foraminiferal change and depositional history across the
515 Cretaceous–Paleogene (K/Pg) boundary in the Brazos River area, Texas: Plymouth
516 University Research Theses, unpublished PhD Thesis (available on the PEARL website).
517 MacLeod, K. G., Whitney, D. L., Huber, B. T., and Koeberl, C., 2007, Impact and extinction in
518 remarkably complete Cretaceous-Tertiary boundary sections from Demerara Rise,
519 tropical western North Atlantic: Geological Society of America Bulletin, v. 119, p. 101–
520 115.
521 Manners, H. R., Grimes, S. T., Sutton, P. A., Domingo, L., Leng, M. J., Twitchett, R. J., Hart, M.
522 B., Dunkley Jones, T., Pancost, R. D., Duller, R., and Lopez-Martinez, N., 2013,
523 Magnitude and profile of organic carbon isotope records from the Paleocene–Eocene
524 Thermal Maximum: Evidence from northern Spain: Earth and Planetary Science Letters,
525 v. 376, p. 220–230.
526 Martinez-Ruiz, F., Bernasconi, S., and McKenzie, J. A., 1994, Paleoceanographic changes across
527 the Cretaceous-Tertiary boundary: carbon and nitrogen isotope stratigraphy:
528 Mineralogical Magazine, v. 58, p. 561–562.
529 Molina, E., Alegret, L., Arenillas, I., Arz, J. A., Gallala, N., Hardenbol, J., Von Salis, K.,
530 Steurbaut, E., Vandenberghe, N., and Zaghbib-Turki, D., 2006, The global boundary
531 stratotype section and point for the base of the Danian Stage (Paleocene, Paleogene,

532 "Tertiary", (Cenozoic) at El Kef, Tunisia – original definition and revision: Episodes, v.
533 29, p., 263–278.
534 Olsson, R. K., Liu, C., and van Fossen, M., 1996, The Cretaceous-Tertiary catastrophic event at
535 Miller's Ferry, Alabama, *in* Ryder, G. et al. (eds.), The Cretaceous-Tertiary boundary
536 event and other catastrophes in earth history: Geological Society of America, Special
537 Paper 307, Boulder, Colorado, p. 263–277.
538 Oxford, M. J., Hart, M. B., and Watkinson, M. P., 2000, Micropalaeontological investigations of
539 the Oxford Clay: Geoscience in south-west England, v. 10, p. 9–13.
540 Oxford, M. J., Hart, M. B., and Watkinson, M. P., 2004, Foraminiferal characterization of mid-
541 Upper Jurassic sequences in the Wessex Basin (United Kingdom): Rivista Italiana di
542 Paleontologia e Stratigrafia, v. 110, p. 209–218.
543 Petrizzo, M. R., 2005, An early late Paleocene event on Shatsky Rise, northwest Pacific Ocean
544 (ODP Leg 198): Evidence for planktonic foraminiferal assemblage, *in* Bralower, T.J.,
545 Premoli Silva, I., & Malone, M.J. (Eds.), Proceedings of the Ocean Drilling Program,
546 Scientific Results, v. 198, p. 1–29.
547 Plummer, H. J., 1926, Foraminifera of the Midway Formation in Texas: University of Texas,
548 Bulletin, no. 2644, 201 p.
549 Plummer, H. J., 1931, Some Cretaceous foraminifera in Texas: University of Texas Bulletin, no.
550 3101, p. 109–203.
551 Pospichal, J. J., 1994, Calcareous nannofossils at the K-Pg boundary El Kef, Tunisia: no
552 evidence for stepwise, gradual or sequential extinctions: Geology, v. 22, p. 99–102.
553 Punekar, J., Mateo, P., and Keller, G., 2014, Effects of Deccan volcanism on paleoenvironment
554 and planktonic foraminifera: A global survey, *in* Keller, G., and Kerr, A. C. (eds.)

555 Volcanism, Impacts, and Mass Extinctions: Causes and Effects: Geological Society of
556 America, Special Paper No. 505, p. 91–116.
557 Quillévéré, F., Norris, R. D., Kroon, D., and Wilson, P. A., 2008, Transient ocean warming and
558 shifts in carbon reservoirs during the early Danian: Earth and Planetary Science Letters,
559 v. 265, p. 600–615.
560 Sampei, Y., and Matsumoto, E., 2001, C/N ratios in a sediment core from Nakaumi Lagoon,
561 southwest Japan – usefulness as an organic source indicator: Geochemical Journal, v. 35,
562 p. 189–205.
563 Schiøler, P., Brinkhuis, H., Roncaglia, L., and Wilson, G. J., 1997, Dinoflagellate biostratigraphy
564 and sequence stratigraphy of the type Maastrichtian (Upper Cretaceous), ENCI quarry,
565 The Netherlands: Marine Micropaleontology, v. 31, p. 65–95.
566 Schnitker, D., 1979,Cenozoic deep water benthic foraminifers, Bay of Biscay, *in* Montadert, L.
567 et al. (eds.), Initial Reports of the Deep Sea Drilling project, U.S. Government Printing
568 Office, Washington D.C., v. 48, p. 377–414.
569 Schoene, B., Samperton, K. M., Eddy, M. P., Keller, G., Adatte, T., Bowring, S. A., Khadri, S. F.
570 R., and Gertsch, B., 2015, U-Pb geochronology of the Deccan Traps and relation to the
571 end-Cretaceous mass extinction: Science, v. 347, p. 182–184.
572 Schulte, P., and Speijer, R., 2009, Late Maastrichtian-Early Paleocene sea level and climate
573 changes in the Antioch Church Core (Alabama, Gulf of Mexico margin, USA): a multi-
574 proxy approach: Geologica Acta, v. 7, 11–34.
575 Schulte, P., and 40 additional authors, 2010, The Chicxulub asteroid impact and mass extinction
576 at the Cretaceous-Paleogene boundary: Science, v. 327, p. 1214–1218.

577 Schumacher, S., Jorissen, F. J., Mackensen, A., Gooday, A. J., and Pays, O., 2010, Onogenetic
578 effects on stable carbon and oxygen isotopes in tests of live (Rose Bengal stained)
579 benthic foraminifera from the Pakistan continental margin: Marine Micropaleontology, v.
580 76, p. 92–103.
581 Speijer, R. P., 2003, Danian–Selandian sea-level change and biotic excursion on the southern
582 Tethyan margin (Egypt), *in* Wings, S. L. et al. (eds.), Causes and consequences of
583 globally warm climates in the Early Paleogene: Geological Society of America, Special
584 Paper, v. 369, p. 275–290.
585 Surlyk, F., Damholt, T., and Bjerager, M., 2006, Stevns Klint, Denmark: Uppermost
586 Maastrichtian chalk, Cretaceous–Tertiary boundary, and lower Danian bryozoans mound
587 complex: Bulletin of the Geological Society of Denmark, v. 54, p. 1–48.
588 Twitchett, R. J., 2006, The palaeoclimatology, palaeoecology and palaeoenvironmental analysis
589 of mass extinction events: Paleogeography, Palaeoclimatology, Palaeoecology, v. 232, p.
590 190–213.
591 Wendler, I., Huber, B. T., MacLeod, K. G., and Wendler, J. E., 2013, Stable oxygen and carbon
592 isotope systematic of exquisitely preserved Turonian foraminifera from Tanzania –
593 understanding isotopic signature in fossils: Marine Micropaleontology, v. 102, p. 1–33.
594 Westerhold, T., Röhl, U., and Laskar, J., 2012, Time scale controversy: Accurate orbital
595 calibration of the early Paleogene: Geochemistry, Geophysics, Geosystems, v. 13,
596 Q06015, DOI: 10.1029/2012GC004096
597 Yancey, T. E., 1996, Stratigraphy and depositional environments of the Cretaceous-Tertiary
598 boundary complex and basal Paleocene section, Brazos River, Texas: Transactions of the
599 Gulf Coast Association of Geological Societies, v. 46, p. 433–442.

Yancey, T. E., and Liu, C., 2013, Impact-induced sediment deposition on an offshore, mud substrate continental shelf, Cretaceous-Paleogene boundary, Brazos River, Texas, USA: Journal of Sedimentary Research, v. 83, p. 354–367.

Zachos, J. C., Pagani, M., Sloan, L., Thomas, E., and Billups, K., 2001, Trends, rhythms, and aberrations in global climate 65 Ma to present: Science, v. 292, p. 686–693.

Zachos, J. C., McCarren, H., Murphy, B., Röhl, U., and Westerhold, T., 2010, Tempo and scale of late Paleocene and early Eocene carbon isotope cycles: Implications for the origin of hyperthermals: Earth and Planetary Science Letters, v. 299, p. 242–249.

Received 25 March 2015

Accepted 22 March 2017

612

613 FIGURE CAPTIONS

614

615 FIGURE 1. Locality map of the Brazos River area, Falls County, Texas (after Hart et al., 2012).

616

617 FIGURE 2. Sedimentary log of the K/Pg boundary succession exposed on the Brazos River at
618 RBS (based on Hart et al., 2012). The thin volcanic ash recorded in the uppermost Maastrichtian
619 of the Cottonmouth Creek succession (Hart et al., 2012) has not been recorded in the RBS
620 succession, despite digging into the Maastrichtian mudstones as far as river levels allowed.

621

622 FIGURE 3. Sedimentary log of the RBS succession, which also shows examples of a
623 representative selection of benthic foraminifera. The lithological symbols are explained in Figure
624 2 and the bed names follow Yancey (1996) including, from bottom to top, Hummocky Cross-
625 Stratification (HCS), Lower Calcareous Horizon (LCH), Middle Sandstone Bed (MSB), Dirty
626 Sandstone Bed (DSB), Upper Calcareous Horizon (UCH) and Rusty Pyrite Horizon (RPH).

627

628 FIGURE 4. Comparison of the $\delta^{18}O$ and $\delta^{13}C$ stable isotope data derived from an analysis of
629 *Lenticulina rotulata* Lamarck in the >500 μm, 500–250 μm and 250–150 μm size fractions. The
630 thinner black line marks the running average.

631

632 FIGURE 5. Bulk organic $\delta^{13}C$, fine fraction $\delta^{18}O/\delta^{13}C$ and C/N ratio data for the RBS succession.
633 The data are plotted against the same sedimentary log as used in Figures 3 and 4 to ease
634 comparison, with the dashed line representing the K/Pg boundary.

635

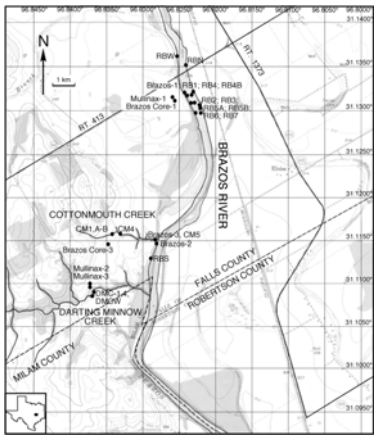

636

637 Figure 1. Locality map of the Brazos River area, Falls County, Texas (after Hart et al., 2012).

638

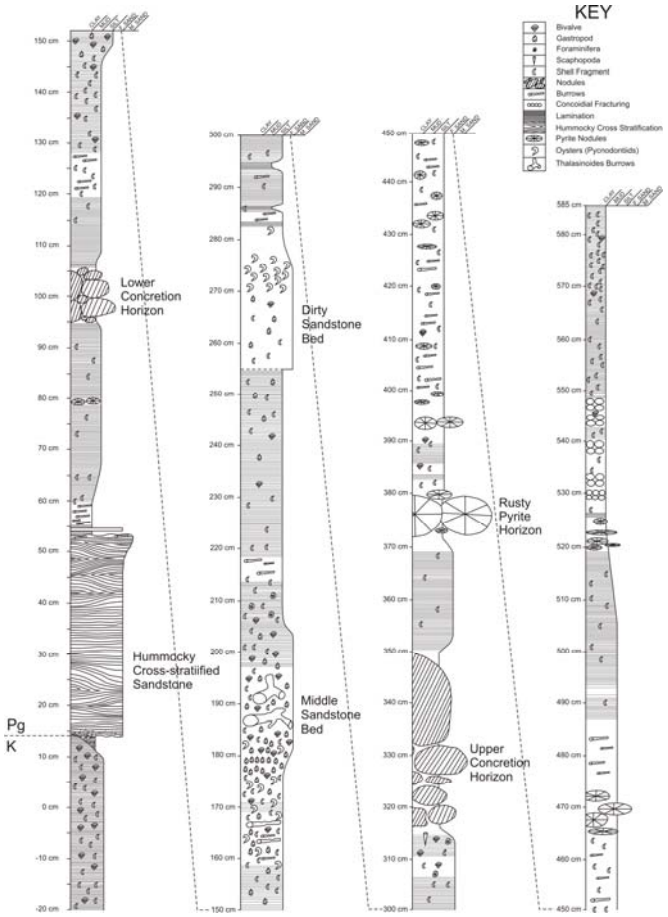

639

Figure 2. Sedimentary log of the K/Pg boundary succession exposed on the Brazos River at RBS (based on Hart et al., 2012). The thin volcanic ash recorded in the uppermost Maastrichtian of the Cottonmouth Creek succession (Hart et al., 2012) has not been recorded in the RBS succession, despite digging into the Maastrichtian mudstones as far as river levels allowed.

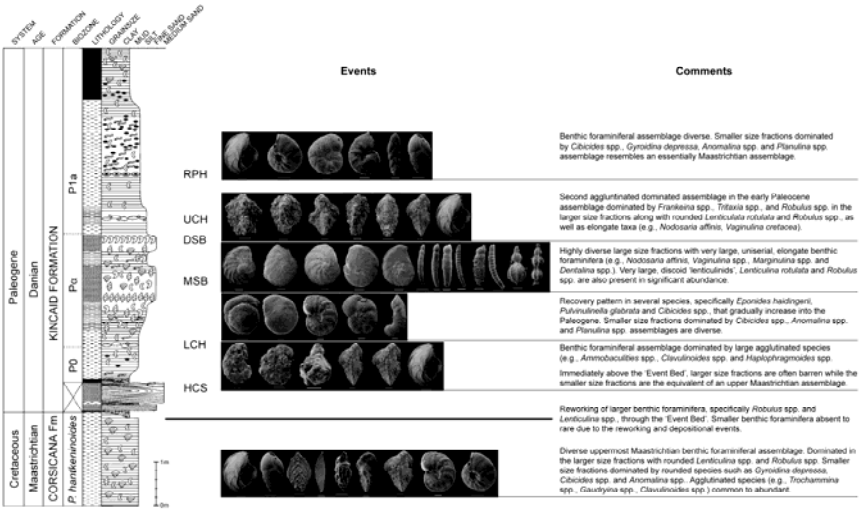

Figure 3. Sedimentary log of the RBS succession, which also shows examples of a representative selection of benthic foraminifera. The lithological symbols are explained in Figure 2 and the bed names follow Yancey (1996) including, from bottom to top, Hummocky Cross-Stratification (HCS), Lower Calcareous Horizon (LCH), Middle Sandstone Bed (MSB), Dirty Sandstone Bed (DSB), Upper Calcareous Horizon (UCH) and Rusty Pyrite Horizon (RPH).

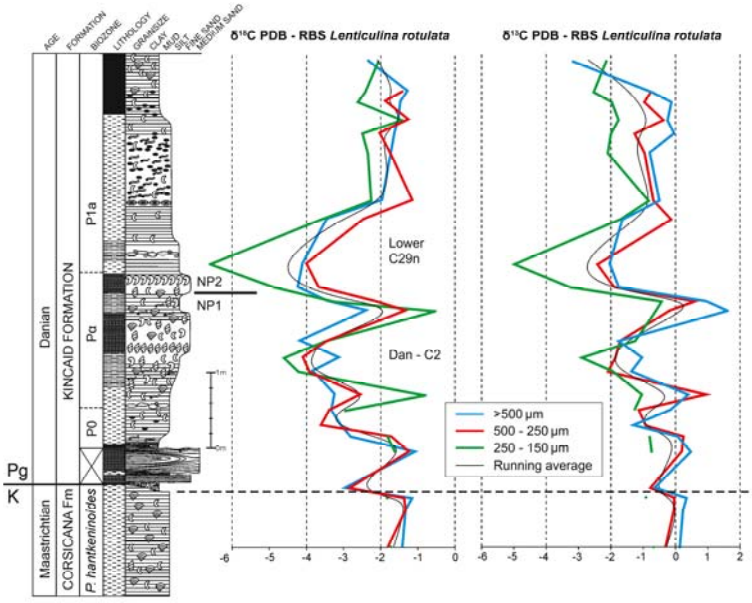

653

654 Figure 4. Comparison of the $\delta^{18}O$ and $\delta^{13}C$ stable isotope data derived from an analysis of

655 *Lenticulina rotulata* Lamarck in the >500 µm, 500–250 µm and 250–150 µm size fractions. The

656 thinner black line marks the running average.

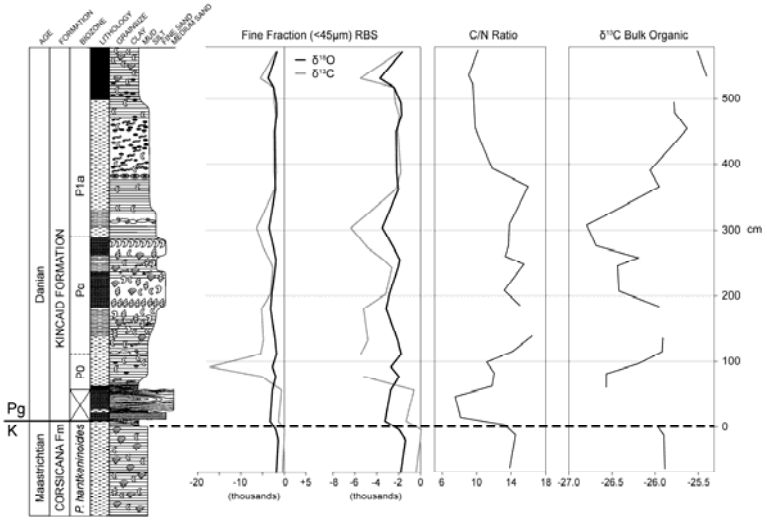

657

658 Figure 5. Bulk organic $\delta^{13}C$, fine fraction $\delta^{18}O/\delta^{13}C$ and C/N ratio data for the RBS succession.

659 The data are plotted against the same sedimentary log as used in Figures 3 and 4 to ease

660 comparison, with the dashed line representing the K/Pg boundary.